

Supporting information

Orange-peel derived carbon loaded low content ruthenium nanoparticles as ultra-high performance alkaline water HER electrocatalysts

Yang Teng, Lu Zhou, Yi-Zhi Chen, Jun-Zhe Gan, Ye Xi, Hai-Lang Jia*

School of Chemistry and Chemical Engineering, Institute of Advanced Functional Materials for Energy, Analysis and Testing Center of Jiangsu University of Technology, Jiangsu University of Technology, Changzhou 213001, P. R. China.

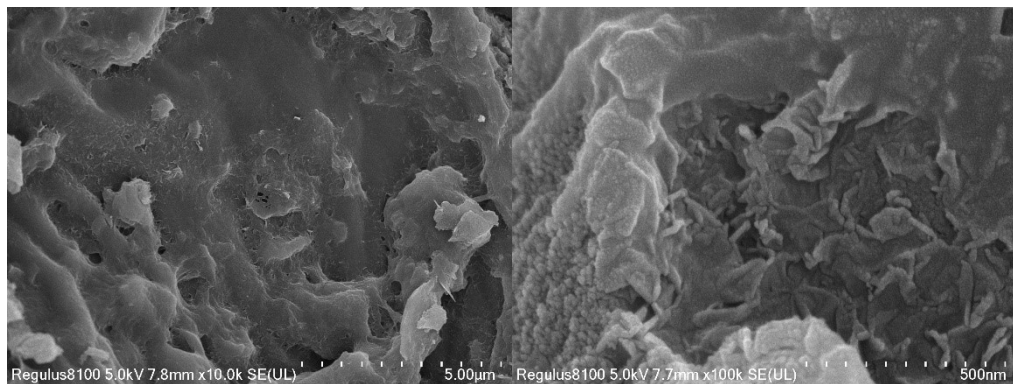


Fig. S1 SEM of OPC

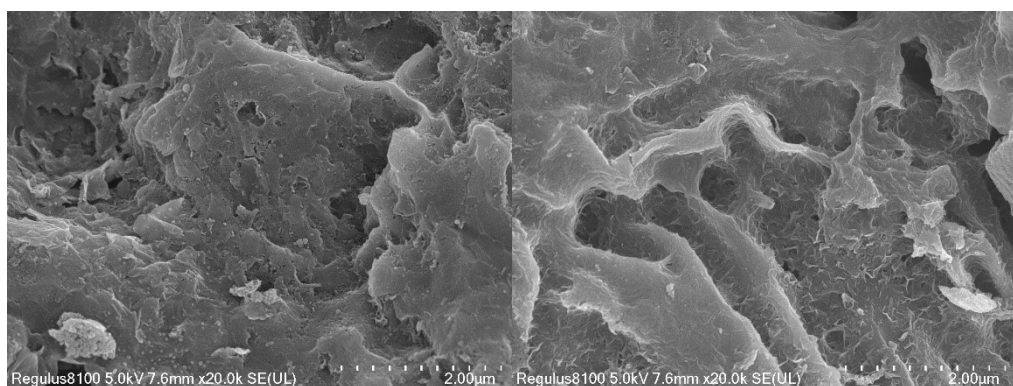
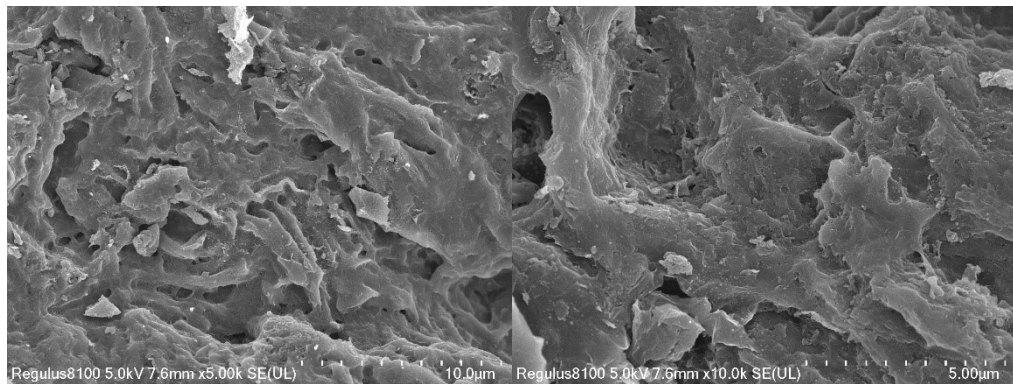


Fig. S2 SEM of Ru/OPC

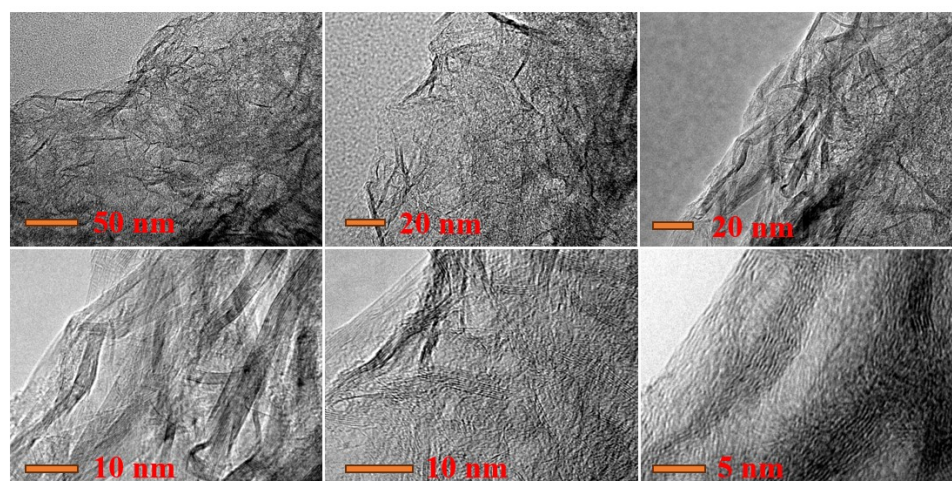


Fig. S3 TEM of OPC

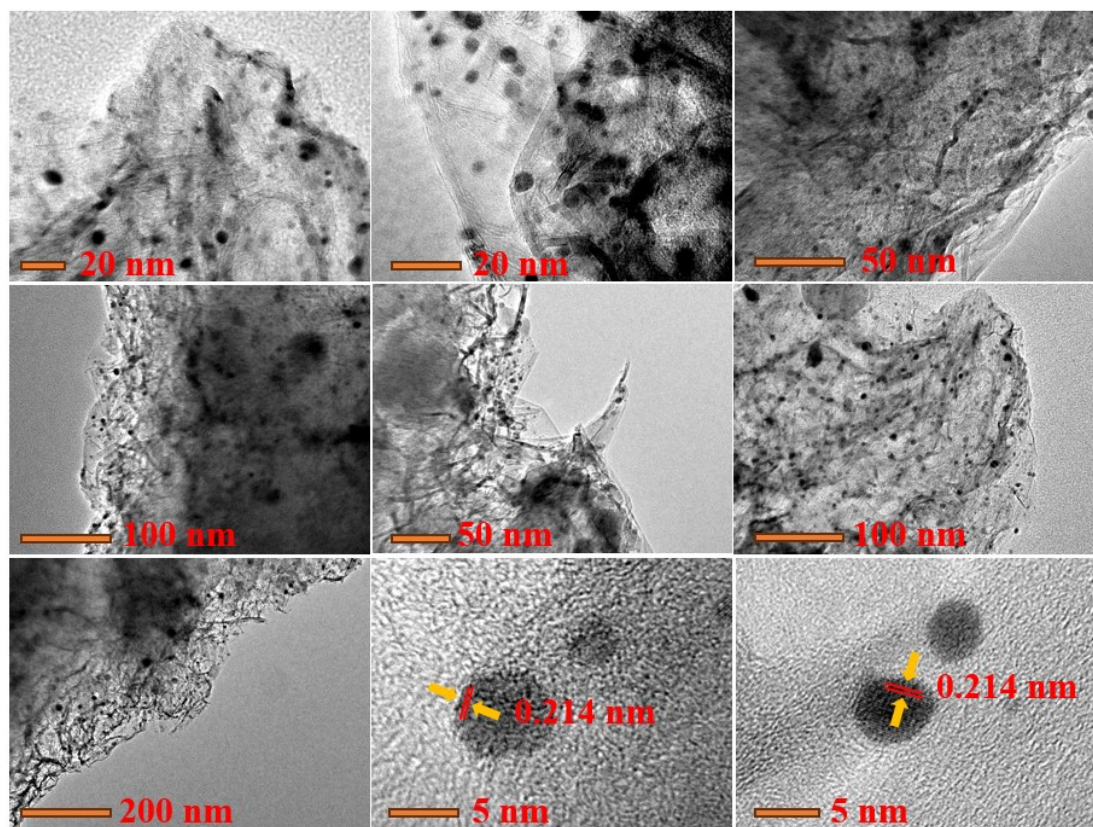


Fig. S4 TEM of Ru/OPC

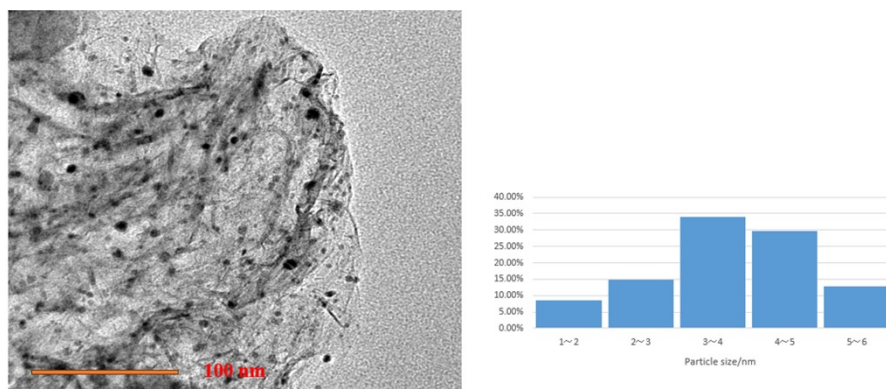


Fig. S5 Particle size distribution of Ru/OPC

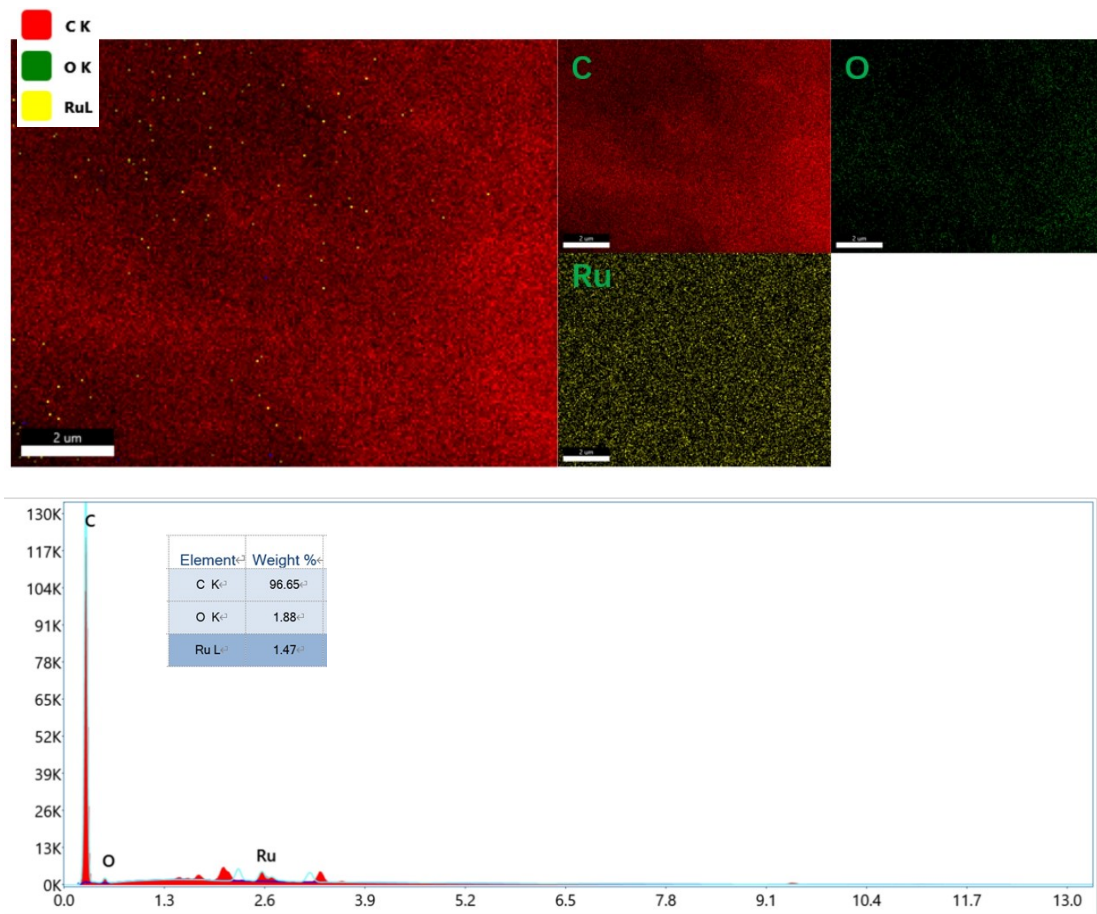


Fig. S6 SEM-EDS mapping of Ru/OPC

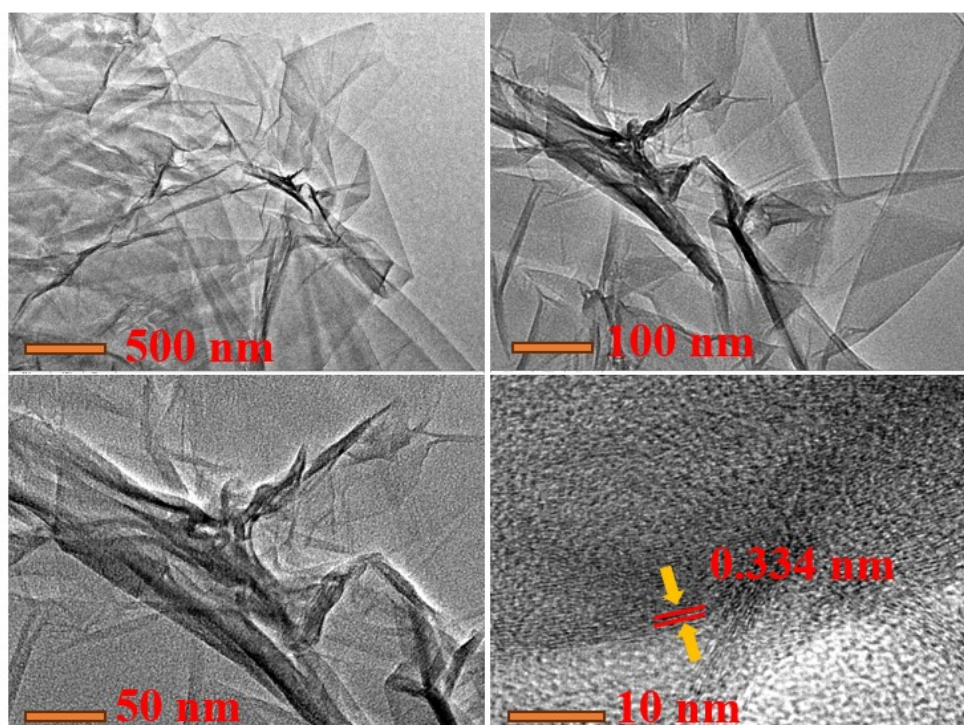


Fig. S7 TEM of rGO

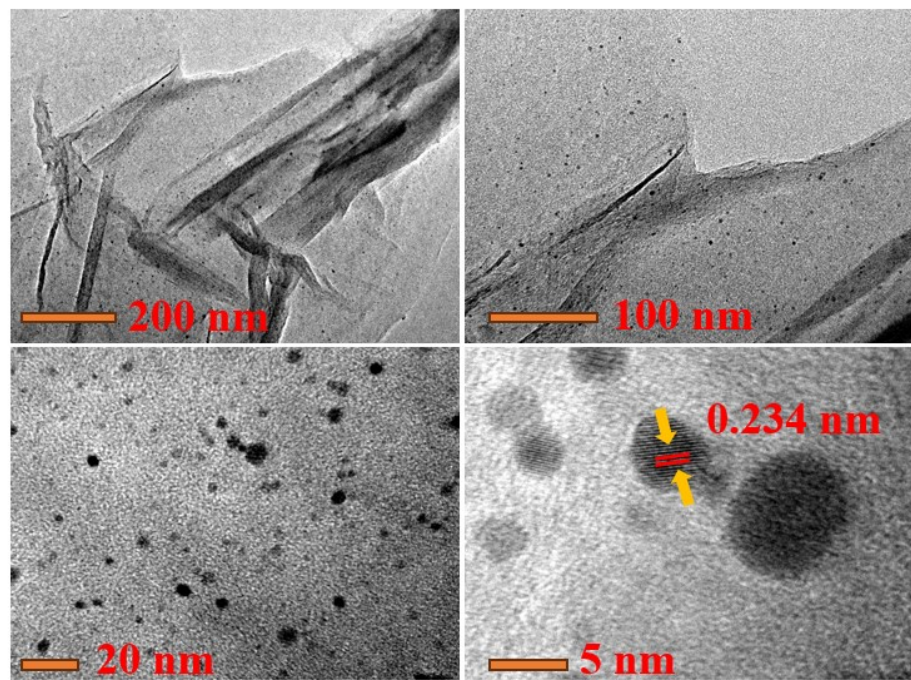


Fig. S8 TEM of Ru/rGO

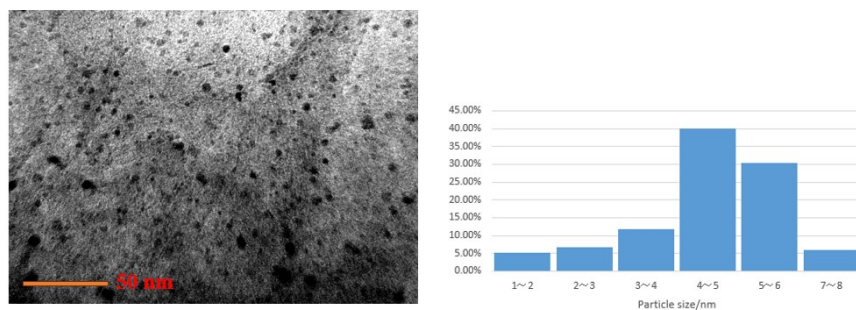


Fig. S9 Particle size distribution of Ru/rGO



Fig. S10 Contact angle of Ru/rGO and Ru/OPC

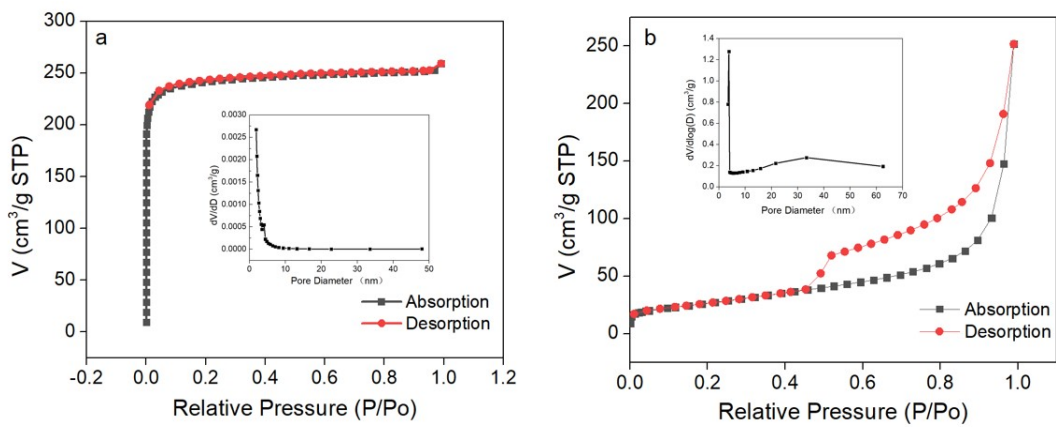


Fig. S11 (a) N₂ adsorption-desorption isotherms and the pore size distribution of Ru/OPC, (b) N₂ adsorption-desorption isotherms and the pore size distribution of Ru/rGO.

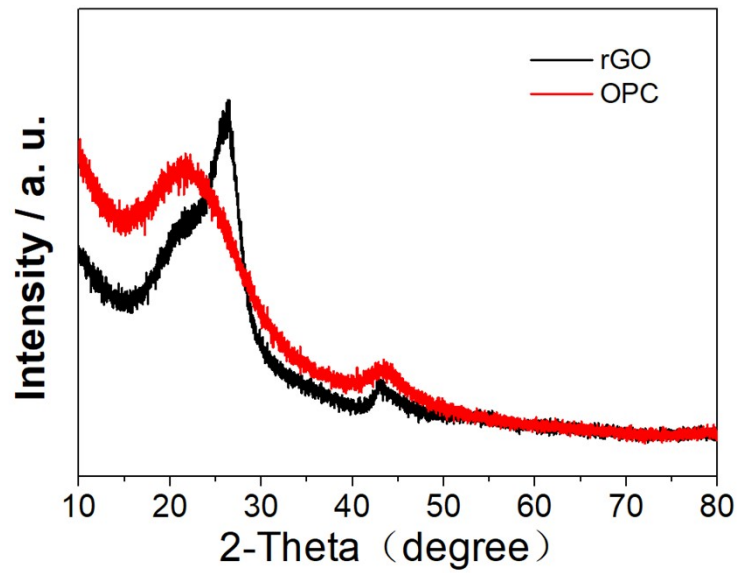


Fig. S12 XRD of rGO and OPC

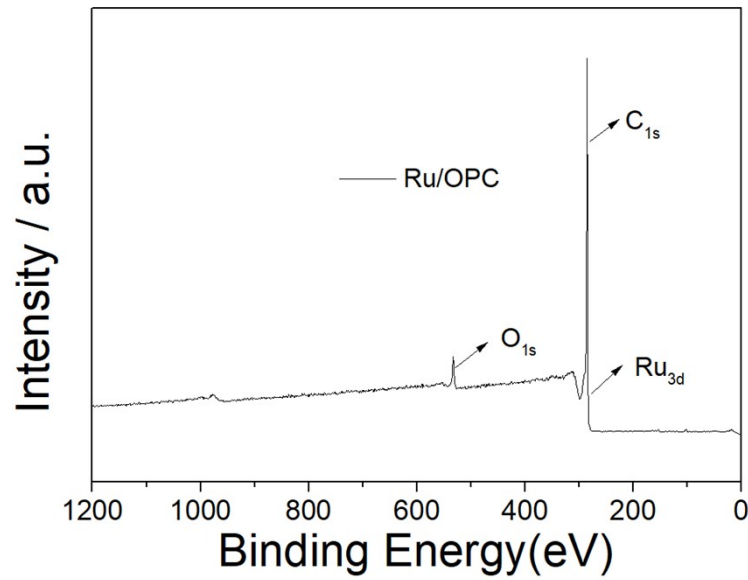


Fig. S13 XPS survey spectra of Ru/OPC

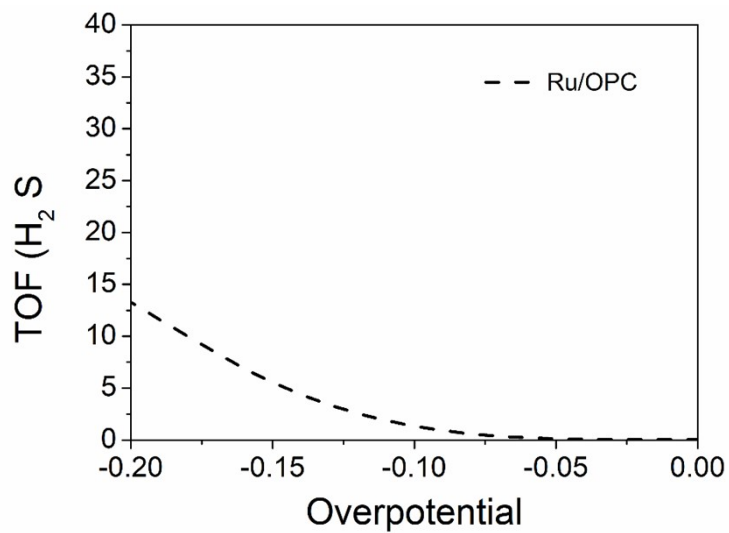


Fig. S14 TOF of Ru/OPC in 0.5 M H₂SO₄

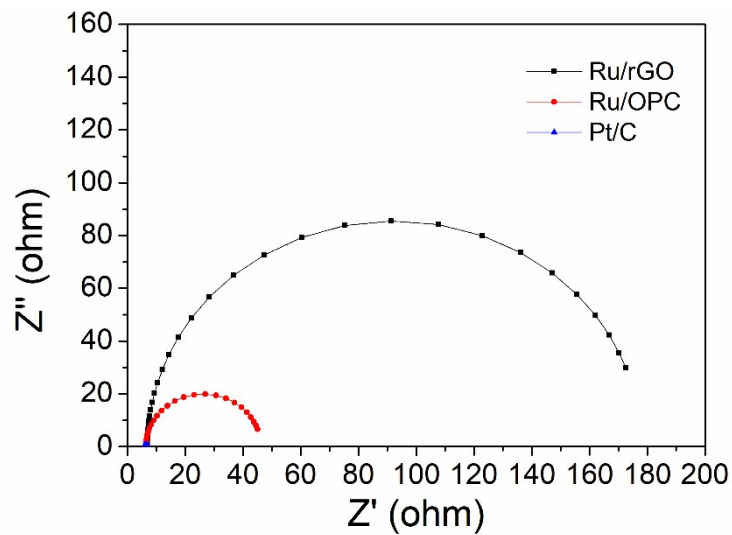


Fig. S15 EIS of Ru/OPC in 0.5 M H_2SO_4

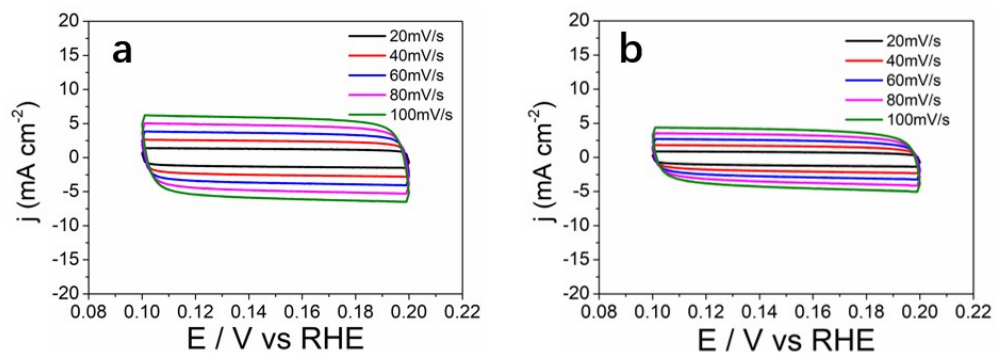


Fig. S16 CV curves of Ru/rGO (a) in 1 M KOH, (b) in 0.5 M H_2SO_4

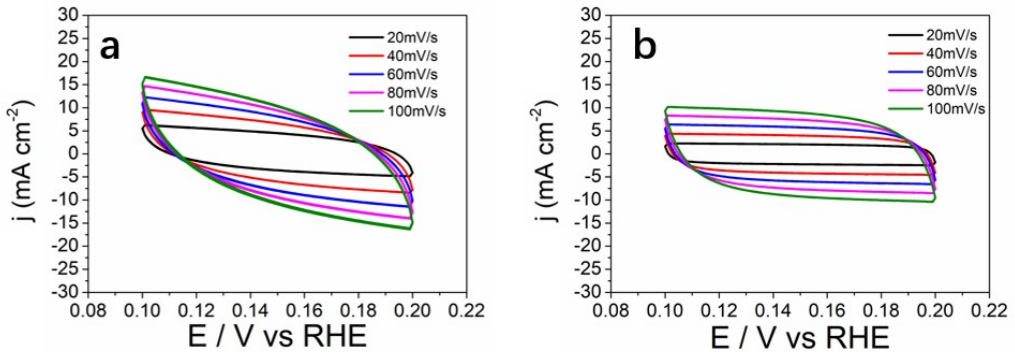


Fig. S17 CV curves of Ru/OPC (a) in 1 M KOH, (b) in 0.5 M H₂SO₄

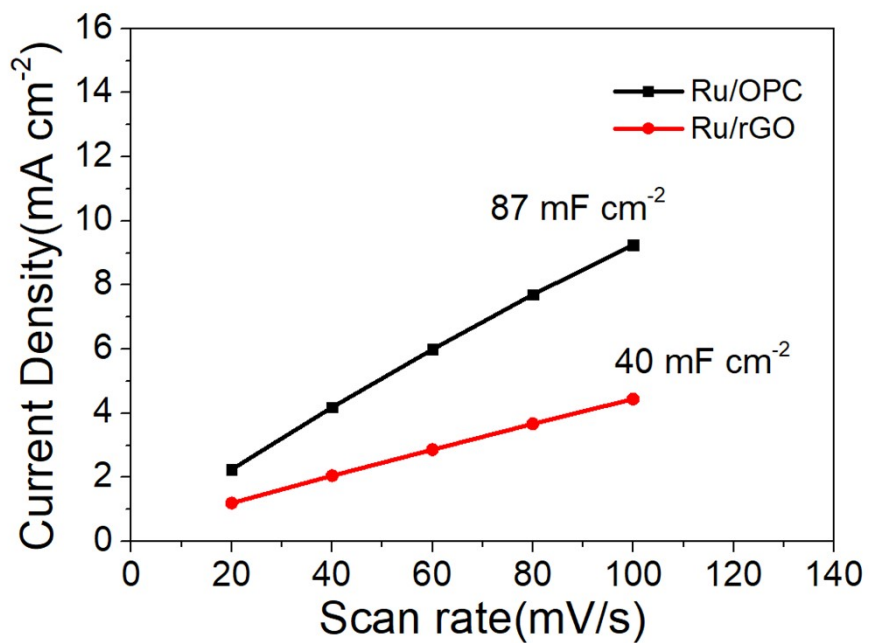


Fig. S18 The linear slope of Ru/rGO and Ru/OPC, equivalent to twice the double-layer capacitance (C_{dl}) in 0.5 M H₂SO₄.

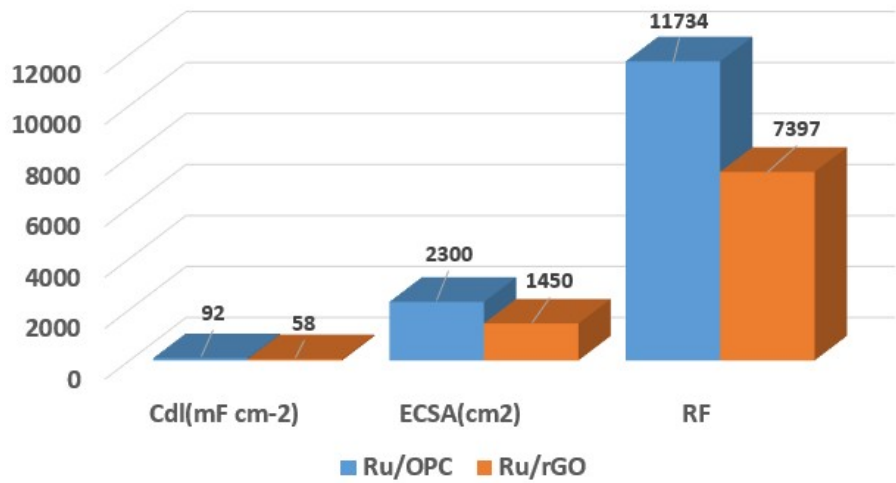


Fig. S19 C_{dl} , ECSA, RF of the Ru/OPC and Ru/rGO in 1 M KOH.

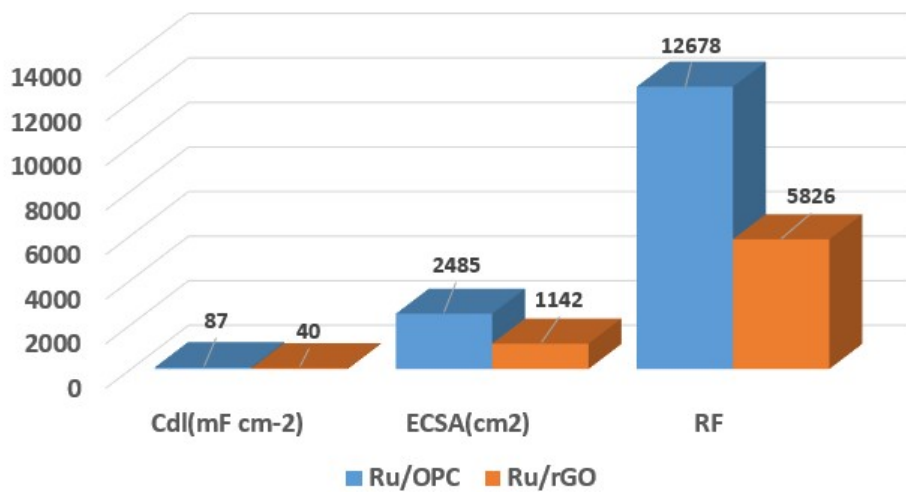


Fig. S20 C_{dl} , ECSA, RF of the Ru/OPC and Ru/rGO in 0.5 M H_2SO_4 .

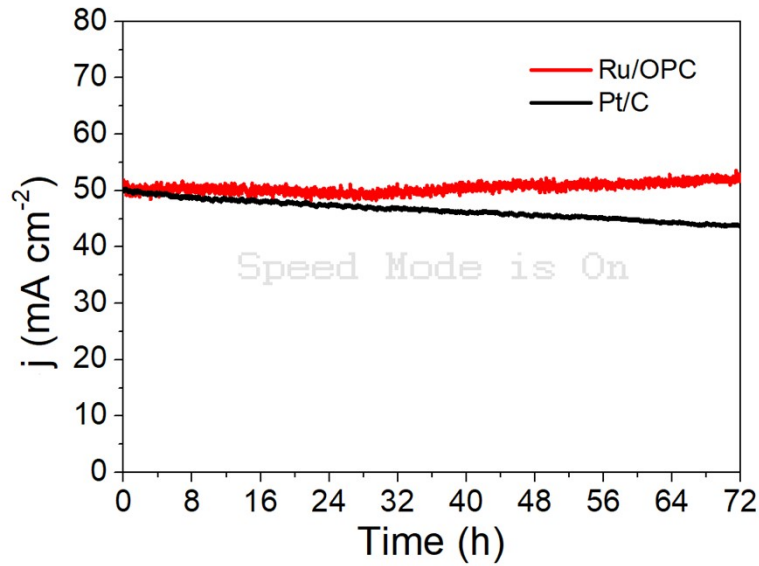


Fig. S21 Long-term i-t response test for Ru/OPC and Pt/C in 0.5 M H_2SO_4 .

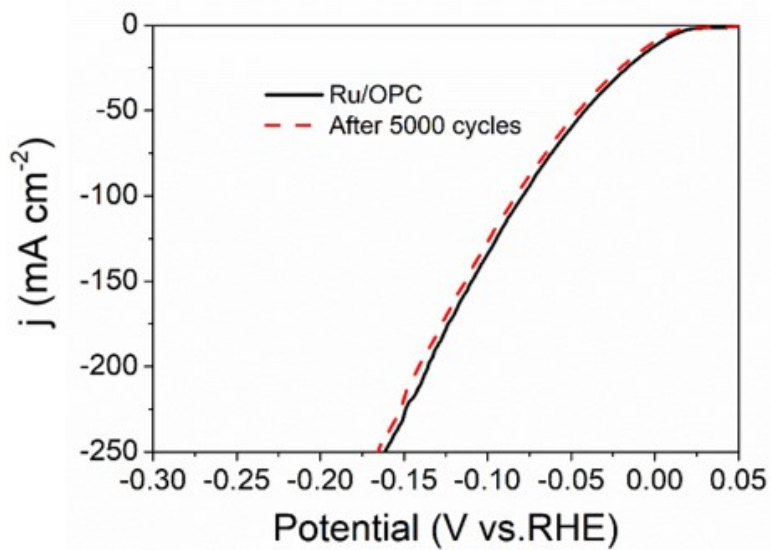


Fig. S22 LSVs of Ru/OPC catalysts before and after 5000 CV cycles in 1 M KOH

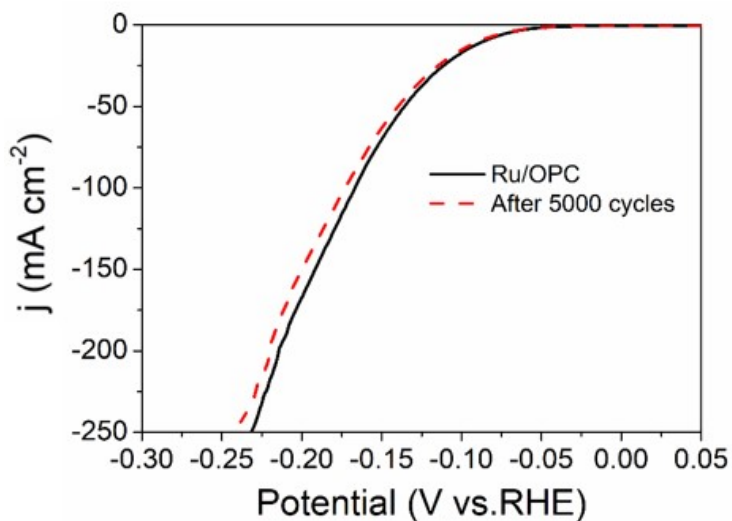


Fig. S23 LSVs of Ru/OPC catalysts before and after 5000 CV cycles in 0.5 M H_2SO_4

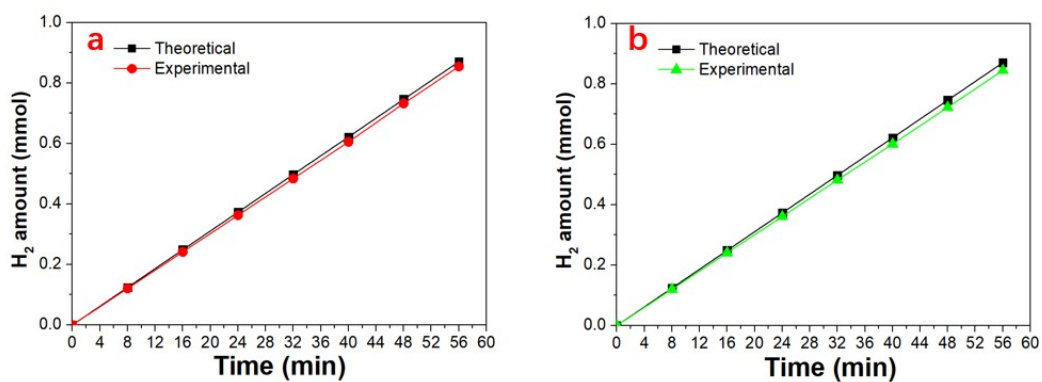


Fig. S24 Faradaic efficiency of Ru/OPC in 1 M KOH (a) and 0.5 M H_2SO_4 (b).

Table S1. Summary of HER catalytic activities of Ru/OPC and some other catalysts reported in recent literatures (1 M KOH).

Catalysts	Overpotential	Tafel Slope (mV dec ⁻¹)	Ref.
Ru/OPC	3 mV at 10 mA cm ⁻²	49	In this work
Ru-CoP/NC	22 mV at 10 mA cm ⁻²	50	ACS Appl. Mater. Interfaces, 2021, 13, 56035–56044.
Ru/C	39 mV at 10 mA cm ⁻²	/	ACS Appl. Energy Mater., 2021, 4, 4284–4289.
CoRu-O/A@HNC-2	85 mV at 10 mA cm ⁻²	72.5	ACS Appl. Mater. Interfaces, 2020, 12, 51437–51447.
Ru@NC	39 mV at 10 mA cm ⁻²	37.9	ACS Sustainable Chem. Eng., 2022, 10, 15530–15537.
ld-Ru@a-Co/Ti	33.5 mV at 10 mA cm ⁻²	39.6	Chem. Commun., 2022, 58, 13588–13591.
Ni2P–Ru/NF	40 mV at 10 mA cm ⁻²	33.9	Sustainable Energy Fuels, 2023, 7, 2830–2840.
Ru/Mo2C@NC	13 mV at 10 mA cm ⁻²	33.2	J. Mater. Chem. A, 2021, 9, 20518–20529.
Ru/PEI-XC	13 mV at 10 mA cm ⁻²	79.3	J. Mater. Chem. A, 2021, 9, 22934–22942.
MoRu/C	27.1 mV at 5 mA cm ⁻²	51	Chem. Commun., 2020, 56, 14475–14478.
D/NFF-Ru-Zn	90 mV at 100 mA cm ⁻²	41	J. Mater. Chem. A, 2022, 10, 20453–20463.
CF@Ru-CoCH NWs	121 mV at 100 mA cm ⁻²	65	Electrochim. Acta, 2020, 331, 135367
Ru/TiOxNy NBs	16 mV at 10 mA cm ⁻²	42	J. Mater. Chem. A, 2022, 10, 11205–11212.
RuCr@C	19 mV at 10 mA cm ⁻²	24	Adv. Funct. Mater., 2021, 32, 2108991.
Ru MNSs	24 mV at 10 mA cm ⁻²	33	Angew. Chem. Int.

			Ed. Engl., 2022, e202116867.
P-Ru-CoNi-LDH	29 mV at 10 mA cm ⁻²	69	Small, 2022, 18, e2104323.
CC@WS2/Ru-450	32.1 mV at 10 mA cm ⁻²	53.2	Adv. Funct. Mater., 2022, 2109439.
Ru-HMT-MP-7	33 mV at 10 mA cm ⁻²	26.4	Small, 2022, e2105168.
Ni5P4-Ru	155 mV at 10 mA cm ⁻²	92	Adv. Mater., 2020, 32, e1906972.
Ru-NiCo2S	32 mV at 10 mA cm ⁻²	41.3	Adv. Funct. Mater., 2021, 2109731.
RuRh-Co	32 mV at 10 mA cm ⁻²	31	Nano Energy, 2021, 90, 106579.